Recording Intracellular Molecular Events from the Outside: Glycosylphosphatidylinositol-Anchored Avidin as a Reporter Protein for In Vivo Imaging

Steffi Lehmann[1], Elisa Garcia Garayoa[2], Alain Blanc[2], Ruth Keist[1], Roger Schibli[2,3], and Markus Rudin[1,4]

[1]*Institute for Biomedical Engineering, ETH Zurich and University of Zurich, Zurich, Switzerland;* [2]*Center for Radiopharmaceutical Science, Paul Scherrer Institute, Villigen, Switzerland;* [3]*Institute for Pharmaceutical Sciences, ETH Zurich, Zurich, Switzerland; and* [4]*Institute of Pharmacology and Toxicology, University of Zurich, Zurich, Switzerland*

With the emergence of multimodal imaging strategies, genetically encoded reporters that can be flexibly combined with any imaging modality become highly attractive. Here we describe the use of glycosylphosphatidylinositol (GPI)-anchored avidin, an avidin moiety targeted to the extracellular side of cell membranes via a GPI anchor, as a reporter for in vivo imaging. Being present on the outside of cells, avidin can be visualized with any type of biotinylated imaging agent, without the requirement that the probe be membrane-permeable. We used the avidin–GPI system to monitor the activity of hypoxia-inducible factors (HIFs)—oxygen-sensing transcription factors, which play a major role in regulating cancer progression—in a mouse tumor allograft model. **Methods:** Mouse C51 cells were stably transfected with pH3SVG, a reporter construct driving the expression of avidin–GPI from an HIF-sensitive promoter. The transfected cells were subcutaneously implanted into BALB/c nude mice. At 10 d after tumor inoculation, mice received an intravenous injection of either alexa-594-biocytin or ^{67}Ga-DOTA-biotin, and tumor HIF activity was imaged using fluorescence reflectance imaging or SPECT. **Results:** In vitro cell experiments demonstrated the functionality and HIF-dependent regulation of the avidin–GPI reporter construct. In vivo, avidin–GPI was targeted specifically in allograft tumors with biotinylated imaging probes using both fluorescence imaging and SPECT. Analysis of the reporter expression pattern on ex vivo tumor tissue sections indicated a good overlap, with areas of hypoxia. **Conclusion:** We have demonstrated the utility of avidin–GPI as a reporter for multimodal in vivo imaging using both a fluorescence and a SPECT approach to assess intracellular oxygen signaling in a mouse tumor model.

Key Words: in vivo imaging; multimodal reporter gene; hypoxia-inducible factors; fluorescence imaging; SPECT

J Nucl Med 2011; 52:445–452
DOI: 10.2967/jnumed.110.082412

In vivo molecular imaging of reporter gene products has gained widespread use in biomedical research for assessing molecular events associated with physiologic and pathologic changes not only in cells but also in live animals. Specific reporter genes have been developed for all methods typically used in preclinical, noninvasive in vivo imaging experiments (*1–3*). Recently, the concept of multimodal imaging has emerged as a strategy to overcome shortcomings of individual modalities and to combine their particular advantages (*4*). Such multimodal imaging approaches have prompted the development of multiplexed reporters, which can be used with different imaging modalities. Fusion constructs combining, for example, optical (bioluminescent and fluorescent proteins) and PET reporters (thymidine kinase) are attractive for both multimodal in vivo imaging and in vitro or ex vivo evaluation of reporter activity (*5–7*). However, large fusion constructs are generally laborious to generate and difficult to stably express in cells or transgenic animals. Moreover, once designed, they are confined to the modalities preset by the reporter. Preferably, a reporter protein originates from a single gene, can be combined with any in vivo imaging modality, and is also amenable to in vitro and ex vivo analyses. In an attempt to meet these requirements we evaluated glycosylphosphatidylinositol-anchored avidin (avidin–GPI) as a reporter system for in vivo imaging (*8,9*). Avidin is a small tetrameric protein characterized by high-affinity binding to biotin (*10,11*), and GPI anchors target proteins to the extracellular side of cell membranes (*12*). Hence in the avidin–GPI system, avidin is presented as antigen on the outer cell surface and can be visualized in vivo with biotinylated imaging probes linked to any kind of reporter moiety. These properties of avidin render the system highly flexible and are particularly attractive for the design of reporter assays reflecting intracellular events because the probes do not need to be membrane-permeable. Development of biotinylated imaging probes is straightforward and has been described for most of the current imaging modalities (*9,13–15*).

We used avidin–GPI to read the transcriptional activity of hypoxia-inducible factors (HIFs) in an in vivo fluores-

Received Aug. 18, 2010; revision accepted Dec. 8, 2010.
For correspondence or reprints contact: Markus Rudin, Institute for Biomedical Engineering, ETH Zurich and University of Zurich, Wolfgang-Paulistrasse 27, 8093 Zurich, Switzerland.
E-mail: rudin@biomed.ee.ethz.ch

cence reflectance and SPECT experiment. HIFs are oxygen-regulated transcription factors that mediate the cellular adaptation to pathophysiologic decreases in oxygen levels (*16*). In tumors, HIFs have been shown to be activated not only by tumor hypoxia but also by hypoxia-independent mechanisms to promote tumor cell survival, angiogenesis, and metastasis (*17,18*). Typically, upregulation of HIF in human cancer patients is associated with more aggressive tumor phenotypes and poor prognosis. Imaging HIF activity in live tumors provides an important tool to further study the mechanisms driving its activation in cancer.

MATERIALS AND METHODS

Generation of pH3SVG Reporter Construct

The avidin–GPI fusion construct (*9*) was cut from pCDNA3.1 using *Hin*dIII and *Xba*I and cloned into pH3SVL (*19*) digested with the same enzymes.

Cell Culture and Dimethyloxalyglycine Treatment

Cells were maintained in Dulbecco's modified Eagle's medium, high glucose, containing a 4.5 mg/mL concentration of glucose (GIBCO; Invitrogen). Culture medium was supplemented with 10% heat-inactivated fetal calf serum, 25 U of penicillin per milliliter, and 25 μg of streptomycin per milliliter (Invitrogen). To induce HIF transcriptional activity under normoxic conditions, cells were treated with dimethyloxalyglycine (1–2 mM; Enzo Life Sciences AG) overnight.

Generation of Stably Transfected Cell Lines

Two stable cell lines were generated by transfecting mouse colon cancer C51 cells either with avidin–GPI-pcDNA3.1 or with pH3SVG in combination with pcDNA3.1 at a ratio of 10:1. Transfections were performed using polyethylenimine (catalog no. 23966; Polysciences) as previously described (*17*). Stable transfectants were selected by adding G418 (400 μg/mL). Resistant, single-cell clones were isolated by limited dilution and screened by immunofluorescence staining for high expression levels of avidin–GPI in the case of the avidin–GPI-pcDNA3.1 transfected cells and high expression levels of avidin–GPI in response to treatment with dimethyloxalyglycine (2 mM, overnight) in the case of the pH3SVG cells.

Immunofluorescence and Alexa-594-Biocytin Stainings of Cells Expressing Avidin–GPI

Stably transfected C51 cells were grown on coverslips in 12-well plates to 80% confluency. For immunofluorescence staining, cells were incubated with an avidin antibody (ab 66751; Abcam) at a dilution of 1/1,000 in Hanks balanced salt solution (HBSS) (GIBCO; Invitrogen) containing 1% bovine serum albumin for 20 min at 37°C. Thereafter, cells were gently rinsed in warm HBSS before being incubated with an alexa-488-antirabbit conjugate (Molecular Probes; Invitrogen) at a dilution of 1:1,000 for 20 min at 37°C to immunodetect membrane-bound avidin–GPI. Finally, cells were washed in HBSS, fixed in 4% paraformaldehyde in phosphate-buffered saline (PBS) for 12 min, washed again, and mounted on microscopic slides using mounting medium containing 4′,6-diamidino-2-phenylindole (Prolong Gold; Invitrogen). For stainings involving alexa-594-biocytin (Molecular Probes; Invitrogen) and alexa-594-cadaverine (Molecular Probes; Invitrogen), both dyes were dissolved in PBS at a final concentration of 200 μM. In this case, after being treated with dimethyloxalyglycine for approximately 12 h (1 mM), the cells were starved for 4 h in Dulbecco's modified Eagle's medium without serum to deplete them of biotin present in the culture medium before staining. Analogous to the immunofluorescence approach, cells were then incubated in HBSS containing 1% bovine serum albumin with either alexa-594 cadaverine (200 μM) or alexa-594-biocytin (200 μM) at a dilution of 1/500 for 20 min at 37°C. After being stained, cells were washed and fixed as described. Costainings using alexa-594-biocytin and an anti-avidin antibody coupled to fluorescein isothiocyanate (FITC) (NB 120-7232; Novus Biologicals) were performed with alexa-594-biocytin (200 μM) at a dilution of 1/500 and the antibody at a dilution of 1/200. All images were acquired with an epifluorescence microscope (Axio Imager.Z1; Zeiss) applying the ApoTome option.

Fluorescent-Activated Cell Sorting (FACS) Analysis

For FACS, stably transfected avidin–GPI-pcDNA3.1, pH3SVG, and C51 control cells were plated in 6-well plates to 80% confluency. Half of the wells were treated with dimethyloxalyglycine (2 mM) overnight. For cellular staining, cells were harvested in 2 mL of nonenzymatic cell dissociation agent (Sigma-Aldrich AG), centrifuged at 1,700 rpm (Megafuge 1.0; Kendro Laboratory Products AG) for 5 min, and washed in PBS followed by centrifugation (1,700 rpm, 5 min). Pellets were resuspended in 100 μL of PBS and added with a pipette to a 96-well plate. After centrifugation, cells were incubated in 100 μL of PBS containing the primary anti-avidin antibody (ab 66751; Abcam) at a dilution of 1/200 for 30 min at 4°C. Subsequently, cells were centrifuged (1,700 rpm, 5 min), washed with PBS, and centrifuged again (1,700 rpm, 5 min) before being incubated with a secondary alexa-488-antirabbit conjugate (Molecular Probes; Invitrogen) at a dilution of 1/500 for 30 min at 4°C. After being centrifuged in a final step (1,700 rpm, 5 min) and washed in PBS, cells were analyzed in the FACS analyzer (BD Biosciences).

In Vivo Allograft Tumor Models

All animal protocols were approved by the Cantonal Veterinary Office in Zurich (license 129/2007 XIMO_Y2) and Aargau. To establish allograft tumors, we subcutaneously injected 10^6 C51 control or stably transfected pH3SVG cells into the flank of 8-wk-old BALB/c nude mice (Charles River Laboratories) for the in vivo fluorescence imaging experiments, respectively, and in the shoulder of CD-1 nude mice (Charles River Laboratories) for the SPECT experiments. Animals were maintained under standard hygienic conditions for the duration of the experiment. Five to 7 d before imaging, animals were fed a biotin-free diet (Harlan). Tumor sizes were monitored by caliper measurements. All animals were sacrificed before tumors reached volumes of 2 cm^3.

In Vivo Fluorescence Imaging

For in vivo fluorescence imaging, animals were gas-anesthetized using 3% isoflurane (MINRAD) and an oxygen–air mixture as carrier gas. Spectral imaging was performed in a fluorescence reflectance imaging system (Maestro 500; Cambridge Research Instruments Inc.) using a bandpass filter for excitation (575–605 nm) and a long-pass filter (645 nm) for detection. Spectrally resolved detection of the fluorescence signal was achieved by the liquid crystal tunable filter built into the system (bandwidth, 20 nm; scanning wavelength range, 400–720 nm). The tunable filter automatically stepped in 10-nm increments from 630 to 850 nm. After acquisition of a precontrast image, animals were administered an intravenous injection of 10 nmoles of alexa-594-

biocytin or alexa-594 cadaverine, respectively. Images were then acquired at 60 min, 90 min, and 24 h after injection. To use the spectral unmixing software provided by the manufacturer (Maestro 500; Cambridge Research Instruments Inc.), the spectra of autofluorescence were derived from an appropriate region on the original, spectral fluorescence images. The pure spectrum of alexa-594 was obtained by imaging a 0.005 mM solution of alexa-594-cadaverine diluted in saline (0.9% NaCl). The alexa-594 and the autofluorescence components in the composite images were spectrally unmixed using the spectral unmixing software. Tumor fluorescence was quantified by calculation of tumor-to-background signal ratios on spectrally unmixed images displaying the alexa-594 component only. Tumor and background regions of interest used for quantification were drawn manually using the Maestro imaging software.

Hoechst Perfusion and Immunofluorescence on Tissue Sections

To analyze hypoxic tumor zones, tumor mice received an intravenous injection of pimonidazole (Hypoxy Probe, 1.2 mg in 100 μL of PBS; Natural Pharmacia International) after the last image acquisition, approximately 24 h after contrast injection. An hour later, animals were intravenously perfused with Hoechst H33342 (0.5 mg/animal; Sigma-Aldrich AG) for 2 min before being killed by cervical dislocation. Tumors were excised, frozen, and sectioned. Cryosections (12 μm) were stained according to standard immunofluorescence procedures. A monoclonal antibody against pimonidazole (FITC-MAb1, Hypoxyprobe-1 kit; Natural Pharmacia International) was used to detect hypoxic zones at a dilution of 1/500.

Labeling of DOTA-Biotin with ^{67}Ga

Twenty microliters of DOTA-biotin (C-100, 1 mM; Macrocyclics) were added to 250 μL of 0.5 M ammonium acetate (pH 5.0) and 50 μL of $^{67}GaCl_3$ (150 MBq). The reaction mixture was then heated to 75°C for 30 min. The labeled product was purified via high-performance liquid chromatography (HPLC) to yield the radiotracer in a final specific activity of 37 MBq/μg. The labeling was checked with reversed-phase HPLC using a Varian ProStar system and a radiomatic Flo-one Detector with γ-flow cells (Packard Canberra). HPLC solvents consisted of CH_3CN plus 0.1% trifluoroacetic acid (solvent A) and H_2O plus 0.1% trifluoroacetic acid (solvent B). The labeling control was performed with a linear gradient of 20% A/80% B to 80% A/20% B in 25 min (1.0 mL/min).

Biodistribution Studies

Female CD-1 *nu/nu* mice (age, 6–8 wk; Charles River Laboratories) were injected subcutaneously in the shoulder with 1×10^6 C51 (transfected with pH3SVG or untransfected controls) tumor cells in 100 μL of PBS. Nine days after tumor implantation, the mice received an intravenous injection of 0.2 MBq of ^{67}Ga-DOTA-biotin. At different times after injection (3 and 24 h), the animals were sacrificed by cervical dislocation. Organs and blood were collected and weighed. Subsequently, radioactivity was measured in a γ-counter. Results are presented as percentage of injected dose per gram of tissue.

Cell-Binding Tests with ^{67}Ga-DOTA-Biotin

Untransfected and transfected (pH3SVG) C51 cells were placed in 6-well cell plates at different concentrations (from 6.25×10^4 to 2×10^6 cells) and incubated overnight in the presence or absence of dimethyloxalyglycine (1 mM). Cells were washed twice with PBS and incubated with ^{67}Ga-DOTA-biotin (2 kBq/well) in medium without supplements for 1 h at 37°C. After 2 washing steps with PBS to eliminate unbound activity, cells were recovered with 1N NaOH. Bound radioactivity was measured in a γ-counter (Cobra II Auto-Gammacounter; Packard Canberra). The experiment was performed twice in triplicate.

Imaging

SPECT/CT images were obtained at 1 h (in vivo) and 3 h (postmortem) after intravenous injection of the ^{67}Ga-DOTA-biotin (1 MBq). Images were obtained on an X-SPECT system (Gamma Medica Inc.) equipped with a single-head SPECT device and a CT device. SPECT data were acquired and reconstructed with LumaGEM (version 5.407; lum_10; Segami Corp.). CT data were acquired by an X-Ray CT system (Gamma Medica Inc.) and reconstructed with the Cobra software (version 4.5.1). SPECT and CT images were fused with IDL Virtual Machine (version 6.0; ITT Visual Information Solutions). Images were arranged with Amira software (version 4.0).

RESULTS

Characterization of HIF-Sensitive Avidin–GPI Reporter Construct

A fusion construct consisting of the gene encoding a full-length avidin, C-terminally linked to the signal sequence for the GPI anchor of the human CD14 receptor (*9*), was used to replace luciferase in pH3SVL, a HIF-sensitive reporter construct described previously by Wanner et al. (*19*). The resulting avidin–GPI reporter pH3SVG (Fig. 1A) drives the expression of avidin–GPI from a minimal SV40 promoter, which is further regulated by 3 hypoxia-response elements, the conserved DNA regulatory elements, bound by HIFs (*20*). The functionality of pH3SVG was analyzed by measuring its expression in stably transfected, single-cell clones of C51 murine colon cancer cells by means of immunofluorescence (Fig. 1B). Whereas avidin is expressed at high levels on the cell membrane in response to treatment with dimethyloxalylglycine (*21*), a compound mimicking hypoxia by inducing the stabilization of HIFs (Fig. 1B, top), only basal expression of the reporter was observed in control conditions (Fig. 1B, bottom). The specific interaction between avidin–GPI and biotinylated probes was demonstrated in pH3SVG-transfected C51 cells treated with dimethyloxalyglycine for 12 h and stained with FITC-coupled antibody-binding avidin (Fig. 1C, first column) and alexa-594-biocytin (Fig. 1C, second column), a fluorescently labeled biotin. The overlay of the 2 images showed colocalization of the fluorescent signals arising from the 2 dyes, FITC and alexa-594 (Fig. 1C, third column). Although the predominant signal was observed on the cell membrane, suggesting that most avidin reporter proteins were present at the cell surface, we also detected intracellular avidin moieties. These may represent internalized reporter units or newly synthesized avidin–GPI proteins being exported to the cell membrane.

Quantitative Assessment of HIF-Dependent Regulation of Avidin Expression in pH3SVG Cells

FACS was performed to quantitatively assess HIF-dependent regulation of avidin–GPI expression in pH3SVG-

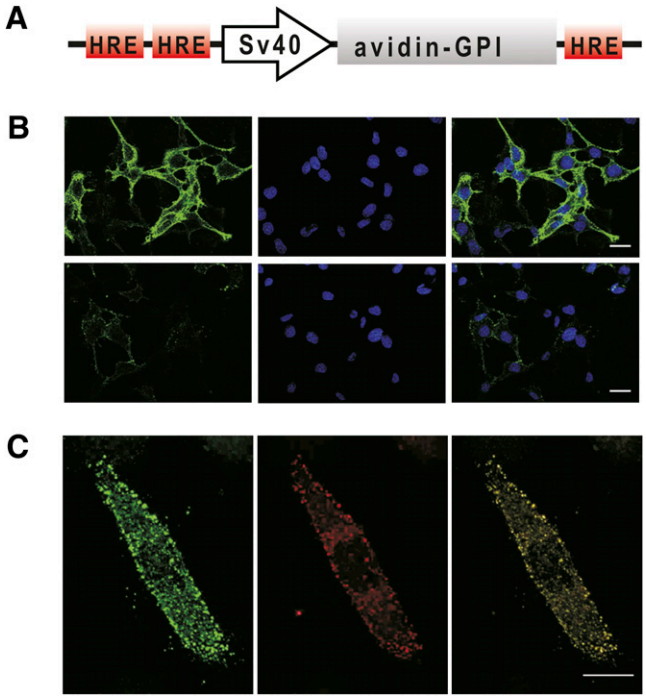

FIGURE 1. Characterization of the avidin–GPI reporter construct (pH3SVG). (A) A schematic drawing of the pH3SVG reporter construct driving the expression of avidin-GPI from a minimal SV40 promoter, further regulated by 3 hypoxia-response elements (HREs). (B) Immunofluorescence staining of a C51 clone, stably expressing pH3SVG. After treatment of cells with dimethyloxalylglycine (top), there was increased expression of avidin–GPI on the cell surface. The first column displays an immunofluorescence staining of avidin, and the second column shows cell nuclei stained with 4′,6-diamidino-2-phenylindole (DAPI);. The third column represents the overlay of the first 2 columns. The scale bar indicates 25 μm. (C) pH3SVG-positive cells treated with dimethyloxalylglycine were simultaneously stained with a FITC-coupled anti-avidin antibody (column 1) and alexa-594-biocytin (column 2). The overlay of the 2 images (column 3) shows colocalization of the 2 stainings. The scale bar is 10 μm.

positive C51 cells. C51 control cells and single-cell clones of cells stably transfected with pH3SVG and avidin–GPI-pcDNA3.1—a control construct driving the expression of avidin–GPI from a constitutively active CMV promoter—were treated with dimethyloxalylglycine for 12 h. Cells were then stained with a fluorescently labeled anti-avidin antibody and subjected to FACS analysis. A shift in fluorescence in response to dimethyloxalylglycine was observed only in the case of the pH3SVG cells (Fig. 2B), whereas there was no significant change in fluorescence intensity in C51 cells (Fig. 2A) and avidin–GPI-pcDNA3.1 cells (Fig. 2C). The geometric means of the fluorescence intensity histograms (Figs. 2A–2C) emphasize the large shift in fluorescence intensity induced by dimethyloxalylglycine in the pH3SVG-transfected cells (Fig. 2D).

In Vivo Fluorescence Imaging of HIF Transcriptional Activity by Targeting Avidin–GPI

For in vivo monitoring of HIF transcriptional activity in a mouse tumor model, C51 control cells and C51 cells stably transfected with the pH3SVG construct were injected subcutaneously into the flank of nude mice. Imaging was performed 10 d after tumor inoculation when tumors had reached diameters of approximately 5–10 mm. In addition to alexa-594-biocytin used to specifically target avidin–GPI, we also used alexa-594-cadaverine as a negative probe, not binding to the surface reporter. Binding of the 2 probes to C51 cells stably expressing pH3SVG after dimethyloxalylglycine stimulation is shown in the supplemental information (Supplemental Fig. 1; supplemental materials are available online only at http://jnm.snmjournals.org). Allograft mice received an intravenous injection of the fluorescent dyes, and the distribution of the dye was monitored after 60 min, 90 min, and 24 h (Fig. 3A). Spectral deconvolution of the images was applied to discriminate signals arising from alexa-594 and unspecific background. Although in animals carrying pH3SVG-positive tumors treated with the biotinylated probe, specific targeting to the tumor site could be observed already at 60 min after injection, this was not the case for pH3SVG tumor animals treated with cadaverine and for mice with C51 control tumors injected with the biotinylated probe. Alexa-594-biocytin showed accumulation in the liver, kidneys, and urinary bladder, consistent with the role of the liver in biotin storage and urinary excretion of this molecule (*22*). Twenty-four hours after injection of the tracer, the main signal detected originated from the kidneys and the tumor, implying that most unbound tracer molecules had been cleared from the circulation. There was some residual fluorescence detected in the gastrointestinal tract, potentially due to autofluorescence of food components. Contrary to this, animals treated with alexa-594-cadaverine did not display any kidney-specific fluorescence, indicating a different excretion mechanism for this compound. The specificity of probe accumulation at the tumor site was analyzed at 24 h after tracer infusion in all 3 study groups. Only for animals carrying pH3SVG C51 tumors injected with alexa-594-biocytin was a fluorescent signal attributable to the dye molecule detected in the tumor region (outlined in red on the whitelight images, Fig. 3B). Neither C51 tumor animals treated with alexa-594-biocytin nor pH3SVG C51 animals dosed with alexa-594-cadaverine displayed a fluorescent signal in the region of interest. Whereas alexa-594-biocytin injection in C51 tumor animals and application of alexa-594-cadaverine to pH3SVG animals did not induce any change in the tumor fluorescence-to-background ratio, the tumor fluorescent signal was clearly increased in pH3SVG animals after injection of the fluorescently labeled biotin (Fig. 3C).

Ex Vivo Analysis of Alexa-594-Biocytin Distribution

The binding specificities of the 2 types of alexa tracers used in the in vivo fluorescence imaging experiments were further assessed ex vivo, on tissue sections (Fig. 4). An alexa-594 fluorescent signal was detected on tumor sections from animals transplanted with pH3SVG-positive cells

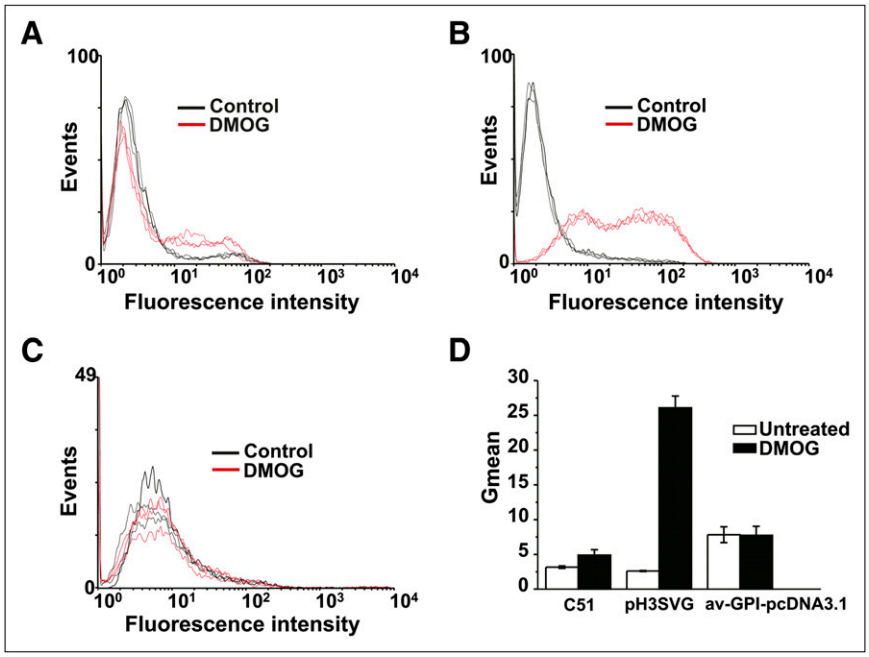

FIGURE 2. FACS analysis to assess HIF-dependent regulation of reporter expression. C51 control cells (A), a C51 clone stably expressing pH3SVG (B), or avidin–GPI pcDNA3.1 (C) were subjected to FACS analysis after treatment with dimethyloxalyglycine. A shift in fluorescence intensity in response to dimethyloxalyglycine treatment was observed only for the pH3SVG cells. (D) Geometric means of the fluorescence intensity histograms (A–C). The geometric mean of pH3SVG cells was significantly increased after dimethyloxalyglycine treatment ($P = 0.00002$). Values are shown as mean ± SD. Av-GPI = avidin–GPI; DMOG = dimethyloxalyglycine.

treated with alexa-594-biocytin. In contrast, no such signal was observed on sections obtained from animals carrying naïve C51 tumors treated with alexa-594-biocytin or from animals with pH3SVG tumors having received alexa-594-cadaverine injections. Comparison of the distribution of alexa-594-biocytin with the uptake pattern of the hypoxia marker pimonidazole (*23*) revealed the association of the HIF activity reporter with regions of hypoxia. Immunofluorescence staining of pimonidazole was particularly strong in regions showing poor tissue perfusion as assessed by intravenous administration of Hoechst H33342, an established histologic perfusion marker (Fig. 4; Supplemental Fig. 2, for the staining of a larger tumor area). Interestingly, the regions positive for alexa-594-biocytin were more extended than those showing increased uptake of pimonidazole. Nitroimidazole-derived compounds such as pimonidazole accumulate in hypoxic cells when partial oxygen pressures decrease to levels that are less than 10 mm Hg (*24*). Thus, cells at the edge of pimonidazole-positive zones may not be hypoxic enough to trap bioreductive, nitroimidazole-derived compounds. Yet, they appear to trigger the stabilization of HIFs and the subsequent activation of the avidin–GPI reporter protein. These findings are in line with earlier observations demonstrating that HIF expression and activity do not necessarily correlate with tumor hypoxia as detected by nitromidazole derivatives (*17*).

In Vivo SPECT Experiments Demonstrate Utility of Avidin–GPI as Multimodal Reporter Protein

To test the feasibility of using avidin–GPI in a nuclear imaging approach, we assessed binding of a biotinylated SPECT probe, ^{67}Ga-DOTA-biotin, to pH3SVG-expressing C51 and C51 control cells (Fig. 5A). Binding of the probe was significantly increased in the case of pH3SVG-expressing cells. Moreover, in line with the responsiveness of the reporter to HIF, binding to these cells could be further potentiated by dimethyloxalyglycine treatment. For biodistribution and in vivo SPECT experiments, tumor allografts were established by injection of C51 control cells in the right shoulder and pH3SVG-transfected cells in the left shoulder of nude mice, respectively. Ten days after tumor inoculation, mice received an intravenous injection of ^{67}Ga-DOTA-biotin. Figure 5B shows the postmortem biodistribution of the radiotracer in different organs at 3 and 24 h after injection. pH3SVG tumors displayed a 3- to 4-fold-higher uptake of ^{67}Ga-DOTA-biotin than C51 control tumors at 3 h after injection. Although the overall activity of the radiotracer at the later time point was reduced in both tumors, it was still higher for the tumors expressing avidin–GPI than for C51 control tumors, suggesting a stable reporter–probe complex. The unbound fraction of the radiotracer was primarily excreted via the kidneys into the urine. In vivo SPECT/CT experiments confirmed specific and increased binding of the radiotracer to pH3SVG-expressing tumor cells (Fig. 5C). The SPECT images showed high activities in the tumors expressing avidin–GPI (left shoulder) both 1 and 3 h after injection, whereas there was only little to no activity detected in the control tumors. In line with the findings obtained from the biodistribution experiments, some tracer uptake was also observed in the kidneys.

DISCUSSION

Imaging the expression of reporter genes is a frequently used strategy in molecular and cellular biology that has been successfully translated to in vivo imaging (*25*). With the emergence of multimodal imaging approaches, strategies based on reporter designs, which are consistent with

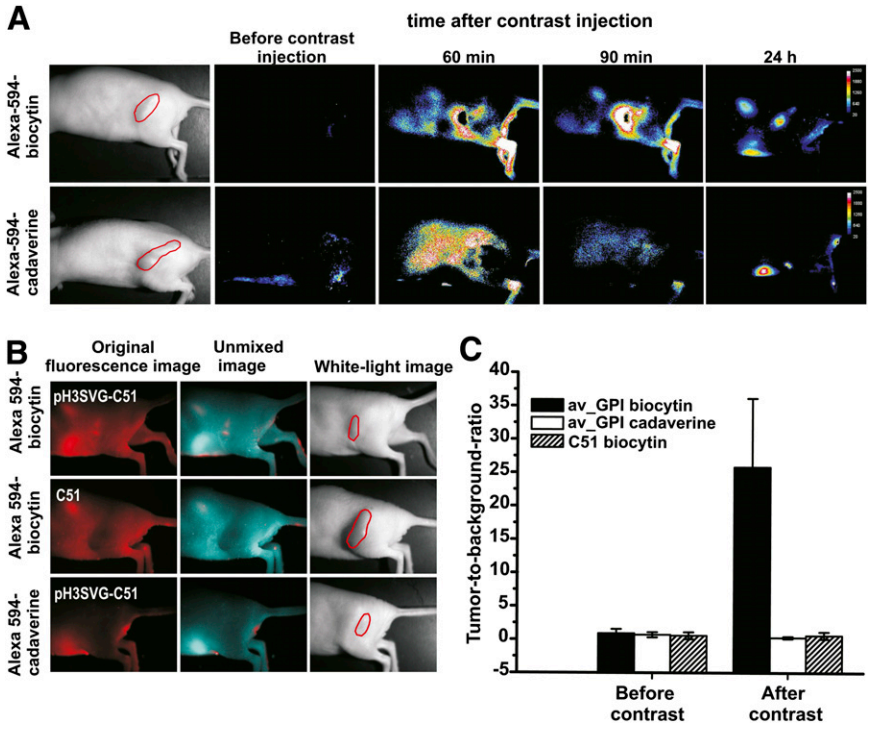

FIGURE 3. In vivo assessment of avidin–GPI reporter activity. (A) In vivo assessment of tumor fluorescence after intravenous injection of either alexa-594-biocytin or alexa-594-cadaverine in pH3SVG tumor animals. Images only show the spectrally unmixed alexa-594 fluorescence component. (B) Original fluorescence, spectrally unmixed, and white light images for pH3SVG animals treated with biocytin or cadaverine and a C51 control animal injected with the biotinylated compound at 24 h after injection. (C) Tumor-to-background ratios calculated on spectrally unmixed fluorescence images. Whereas this ratio did not change for control animals, there was increased tumor fluorescence in pH3SVG tumors at 24 h after injection of the dye. The high variability between animals may reflect different degrees of hypoxia in the analyzed tumors. Values are shown as mean ± SD.

different imaging modalities, are gaining increasing interest. Multimodal properties of imaging probes can be readily achieved by linking target-specific ligands to contrast moieties such as fluorescent dyes, radionuclides, or para- and superparamagnetic contrast agents for MRI. Typically such probes target proteins at the cell surface or in the extracellular space. A critical step to obtaining specific information is the uniqueness of the molecular target for a specific molecular process or cell type. On the basis of these considerations we have evaluated avidin–GPI, an avidin moiety present on the outer cell surface of stably transfected tumor cells, as a reporter protein for multimodal in vivo imaging. Avidin–GPI is not expressed by mammalian cells and has to be introduced as a transgene analogous to classic reporter genes used in in vivo imaging studies (*26*). By expressing the construct under the control of a promoter of interest (e.g., proteins involved in signal transduction), information on intracellular processes can be read from the cell surface. The avidin reporter is detected with targeted exogenous imaging probes comprising the high-affinity ligand biotin linked to an imaging moiety compatible with a particular imaging modality.

We have demonstrated the feasibility of using avidin–GPI as a reporter for in vivo imaging of the transcriptional activity of HIFs in a fluorescence reflectance and a nuclear imaging (SPECT) approach. In vitro validation of reporter expression showed predominant localization of avidin to the cell membrane and regulation in an HIF-dependent manner. In vivo, in a mouse allograft model, fluorescently labeled and radiolabeled biotin bound specifically to tumor

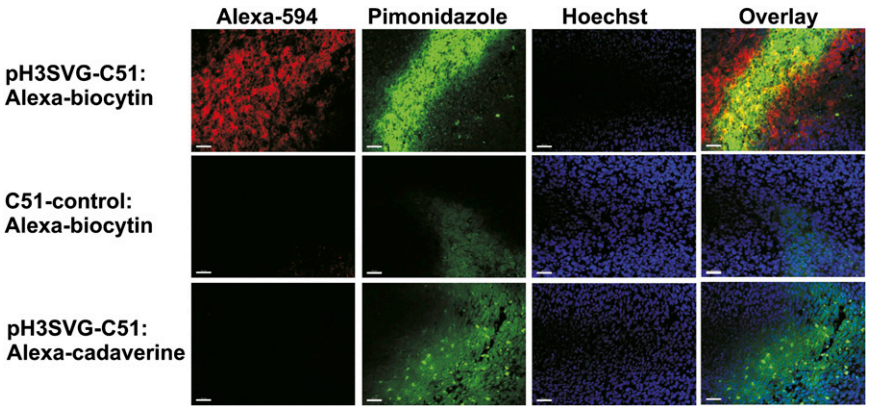

FIGURE 4. Analysis of ex vivo tumor sections showing distribution of alexa-594-biocytin in tumor sections extracted from animals carrying pH3SVG tumors treated with fluorescent biocytin or cadaverine and animals carrying C51 tumors injected with alexa-594-biocytin. Red fluorescence in tumor sections was observed only for pH3SVG animals injected with the biotinylated compound. When analyzing the distribution patterns of the dye and pimonidazole, a marker of hypoxia, we found a good overlap, implying that the reporter activity is increased in hypoxic areas. However, the staining pattern of alexa-594-biocytin extended regions positive for pimonidazole. The scale bar indicates 40 μm.

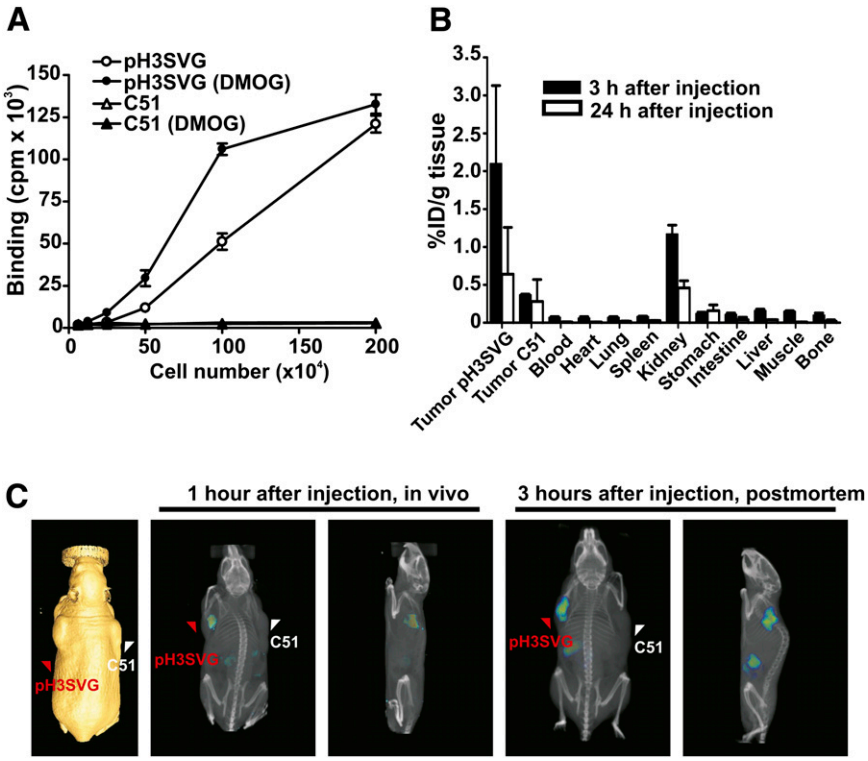

FIGURE 5. In vivo SPECT imaging of avidin–GPI expression. (A) A cell-binding assay demonstrated specific binding of ^{67}Ga-DOTA-biotin to pH3SVG-transfected tumor cells. Dimethyloxalyglycine (DMOG) treatment further potentiated probe binding to these cells. (B) Biodistribution experiments after intravenous injection of ^{67}Ga-DOTA-biotin showed higher tracer uptake in tumors expressing avidin–GPI than in C51 control tumors. This difference in uptake is present at both 3 and 24 h after probe injection. The uptake is displayed as percentage of injected dose normalized to weight of tissue (%ID/g). Values are shown as mean + SD. (C) In vivo SPECT/CT scans confirmed the utility of ^{67}Ga-DOTA-biotin in targeting tumor cells expressing avidin–GPI in vivo. Whereas high activity was detected in positive tumors, the signal arising from negative control tumors of similar size was weak. The tumor surfaces are visualized on an isosurface CT image and marked with arrowheads.

cells expressing avidin–GPI. Nonbound imaging probe was rapidly cleared from the circulation, resulting in a high target-to-background ratio.

With tumor hypoxia and HIFs playing an important role in the regulation of cancer progression, there is an increased demand for the development of tools that allow accurate visualization of tumor hypoxia and HIF transcriptional activity (*27–29*). Several reports have described the development of HIF-responsive genetic reporters to monitor this factor's activity in vivo (*30,31*). However, these experiments have been performed mainly with intracellular, single-gene reporters or reporter fusions that can be combined only with the modalities preset by the reporter proteins. In contrast, our approach allows flexible combination of HIF imaging with any given method and can hence be easily adjusted to any specific biologic question. In a more recent study, the oxygen-dependent degradation domain of HIF-α proteins was fused to streptavidin and a protein transduction domain, mediating cellular uptake of the fusion construct, to monitor HIF-positive tumor cells (*32*). Although based on the flexible avidin–biotin system, too, this reporter can only be targeted with membrane-permeable imaging probes because of its intracellular localization.

In addition to its compatibility with in vivo imaging, the avidin–GPI reporter gene assay lends itself to histologic evaluations, which are essential for validation of in vivo findings. To assess the link between HIF activity and tumor hypoxia, we compared the distribution of the injected fluorescent dye with an immunofluorescence staining of the hypoxia marker pimonidazole on ex vivo tumor sections. We observed a high degree of overlap between pimonidazole-positive tumor regions and tumor regions that were positive for avidin–GPI, that is, all pimonidazole-positive areas were also binding the biotinylated dye. However, avidin–GPI expression was also detected in cells that show poor uptake of pimonidazole—results in line with previous findings demonstrating that the degree of hypoxia as measured with nitroimidazole derivatives and the activity of HIF do not necessarily correlate (*17,33*).

CONCLUSION

We have described a membrane-anchored avidin–GPI reporter system for in vivo imaging of molecular processes in intact organisms. By using a reporter protein that is targeted to the outer cell membrane, it is possible to study intracellular molecular targets without the need for imaging probes to cross the cell membrane. The availability of a ligand, biotin, with high affinity for the reporter protein enables a modular design of imaging probes compatible with the different modalities used in molecular imaging.

ACKNOWLEDGMENTS

We thank Christine De Pasquale and Olga Gasser (Paul Scherrer Institute, Switzerland) for excellent technical support in the SPECT studies; Prof. Shimon Weiss, Dr. Fabien Pinaud, and Dr. Gopal Iyer (Department of Chemistry and Biochemistry, University of California Los Angeles) for

providing the initial avidin–GPI construct and helping with the immunofluorescence staining protocols; and Margarita Plesko and Prof. Christoph Renner (Department for Oncology, University Hospital of Zurich) for their assistance in the FACS experiments. This work was supported by the Swiss National Science Foundation and the National Competence Center for Research (NCCR) Neural Plasticity and Repair.

REFERENCES

1. Kang JH, Chung JK. Molecular-genetic imaging based on reporter gene expression. *J Nucl Med.* 2008;49(suppl):164S–179S.
2. Troy T, Jekic-McMullen D, Sambucetti L, Rice B. Quantitative comparison of the sensitivity of detection of fluorescent and bioluminescent reporters in animal models. *Mol Imaging.* 2004;3:9–23.
3. Gilad AA, Ziv K, McMahon MT, et al. MRI reporter genes. *J Nucl Med.* 2008;49:1905–1908.
4. Cherry SR. Multimodality imaging: Beyond PET/CT and SPECT/CT. *Semin Nucl Med.* 2009;39:348–353.
5. Jacobs A, Tjuvajev JG, Dubrovin M, et al. Positron emission tomography-based imaging of transgene expression mediated by replication-conditional, oncolytic herpes simplex virus type 1 mutant vectors in vivo. *Cancer Res.* 2001;61: 2983–2995.
6. Ray P, De A, Min JJ, Tsien RY, Gambhir SS. Imaging tri-fusion multimodality reporter gene expression in living subjects. *Cancer Res.* 2004;64:1323–1330.
7. Ray P, Wu AM, Gambhir SS. Optical bioluminescence and positron emission tomography imaging of a novel fusion reporter gene in tumor xenografts of living mice. *Cancer Res.* 2003;63:1160–1165.
8. Pinaud F, Michalet X, Iyer G, et al. Dynamic partitioning of a glycosyl-phosphatidylinositol-anchored protein in glycosphingolipid-rich microdomains imaged by single-quantum dot tracking. *Traffic.* 2009;10:691–712.
9. Pinaud F, King D, Moore H-P, Weiss S. Bioactivation and cell targeting of semiconductor CdSe/ZnS nanocrystals with phytochelatin-related peptides. *J Am Chem Soc.* 2004;126:6115–6123.
10. Green NM. Avidin and streptavidin. *Methods Enzymol.* 1990;184:51–67.
11. Laitinen OH, Hytonen VP, Nordlund HR, Kulomaa MS. Genetically engineered avidins and streptavidins. *Cell Mol Life Sci.* 2006;63:2992–3017.
12. Kinoshita T, Fujita M, Maeda Y. Biosynthesis, Remodelling and functions of mammalian GPI-anchored proteins: recent progress. *J Biochem.* 2008;144: 287–294.
13. Amstad E, Zurcher S, Mashaghi A, et al. Surface functionalization of single superparamagnetic iron oxide nanoparticles for targeted magnetic resonance imaging. *Small.* 2009;5:1334–1342.
14. Shoup TM, Fischman AJ, Jaywook S, et al. Synthesis of fluorine-18-labeled biotin derivatives: biodistribution and infection localization. *J Nucl Med.* 1994;35:1685–1690.
15. van Tilborg GA, Mulder WJ, van der Schaft DW, et al. Improved magnetic resonance molecular imaging of tumor angiogenesis by avidin-induced clearance of nonbound bimodal liposomes. *Neoplasia.* 2008;10:1459–1469.
16. Semenza GL. Regulation of mammalian O2 homeostasis by hypoxia-inducible factor 1. *Annu Rev Cell Dev Biol.* 1999;15:551–578.
17. Lehmann S, Stiehl DP, Honer M, et al. Longitudinal and multimodal in vivo imaging of tumor hypoxia and its downstream molecular events. *Proc Natl Acad Sci USA.* 2009;106:14004–14009.
18. Pouyssegur J, Dayan F, Mazure NM. Hypoxia signalling in cancer and approaches to enforce tumour regression. *Nature.* 2006;441:437–443.
19. Wanner RM, Spielmann P, Stroka DM, et al. Epolones induce erythropoietin expression via hypoxia-inducible factor-1 alpha activation. *Blood.* 2000;96: 1558–1565.
20. Wenger RH, Stiehl DP, Camenisch G. Integration of oxygen signaling at the consensus HRE. *Sci STKE.* 2005 Oct 18;2005(306):re12.
21. Jaakkola P, Mole DR, Tian Y-M, et al. Targeting of HIF-alpha to the von Hippel-Lindau ubiquitylation complex by O2-regulated prolyl hydroxylation. *Science.* 2001;292:468–472.
22. Zempleni J, Wijeratne SS, Hassan YI. Biotin. *Biofactors.* 2009;35:36–46.
23. Raleigh JA, Dewhirst MW, Thrall DE. Measuring tumor hypoxia. *Semin Radiat Oncol.* 1996;6:37–45.
24. Gross MW, Karbach U, Groebe K, Franko AJ, Mueller-Klieser W. Calibration of misonidazole labeling by simultaneous measurement of oxygen tension and labeling density in multicellular spheroids. *Int J Cancer.* 1995;61:567–573.
25. Rudin M, Rausch M, Stoeckli M. Molecular imaging in drug discovery and development: potential and limitations of nonnuclear methods. *Mol Imaging Biol.* 2005;7:5–13.
26. Serganova I, Mayer-Kukuck P, Huang R, Blasberg R. Molecular imaging: reporter gene imaging. *Handb Exp Pharmacol.*2008;(185 Pt 2):167–223.
27. Brahimi-Horn MC, Chiche J, Pouyssegur J. Hypoxia and cancer. *J Mol Med.* 2007;85:1301–1307.
28. Harris AL. Hypoxia: a key regulatory factor in tumour growth. *Nat Rev Cancer.* 2002;2:38–47.
29. Semenza GL. Targeting HIF-1 for cancer therapy. *Nat Rev Cancer.* 2003;3: 721–732.
30. Liu J, Qu R, Ogura M, et al. Real-time imaging of hypoxia-inducible factor-1 activity in tumor xenografts. *J Radiat Res (Tokyo).* 2005;46:93–102.
31. Hsieh C-H, Kuo J-W, Lee Y-J, et al. Construction of mutant TKGFP for real-time imaging of temporal dynamics of HIF-1 signal transduction activity mediated by hypoxia and reoxygenation in tumors in living mice. *J Nucl Med.* 2009;50: 2049–2057.
32. Ueda M, Kudo T, Kuge Y, et al. Rapid detection of hypoxia-inducible factor-1-active tumours: pretargeted imaging with a protein degrading in a mechanism similar to hypoxia-inducible factor-1α. *Eur J Nucl Med Mol Imaging.* 2010;37: 1566–1574.
33. Bussink J, Kaanders JHAM, van der Kogel AJ. Tumor hypoxia at the micro-regional level: clinical relevance and predictive value of exogenous and endogenous hypoxic cell markers. *Radiother Oncol.* 2003;67:3–15.